Article

Effects of Changes in Physical Properties of Porous Media and Fluid under Supercritical CO$_2$ Huff-n-Puff in Low-Permeability Reservoir

Guohui Qu *, Xuebin Tian, Yikun Liu, Bowen Li and Xiunan Li

Key Laboratory for Oil and Gas Recovery Improvement of the Ministry of Education, Northeast Petroleum University, Daqing 163000, China; 218003020722@stu.nepu.edu.cn (X.T.); liuyikun@nepu.edu.cn (Y.L.); 228002020098@stu.nepu.edu.cn (B.L.); 228002020095@stu.nepu.edu.cn (X.L.)
* Correspondence: quguohui@nepu.edu.cn

Abstract: The low-permeability reservoirs have abundant reserves and broad development prospects, and the supplementary energy methods have gradually become a hot research topic. In addition, the technology of enhanced oil recovery through supercritical CO$_2$ injection is becoming increasingly mature; however, the changes in reservoir properties at the microscopic level still need further investigation. In this study, natural rock cores from low-permeability reservoirs were used to simulate reservoir conditions and conduct supercritical CO$_2$ injection experiments for energy supplementation. The study aimed to investigate the changes in reservoir microstructure, minerals, and crude oil properties before and after the experiments. The research results indicate that after supercritical CO$_2$ injection into the reservoir, it dissolves in the formation water to form carbonic acid. Under the effect of dissolution, the porosity of the low-permeability reservoir increases by 1.06–5.68%, and permeability can be improved by 40–60%. The rock becomes more water-wet and less oil-wet. The content of calcite and feldspar in the rock minerals decreases due to the dissolution of carbonic acid, resulting in a reduction in plagioclase and calcite. After the CO$_2$ injection, the light components (C$_8$–C$_{10}$) in the crude oil in the rock cores decreased by approximately 14.6%, while the heavy components (C$_{16}$–C$_{39}$) increased by 6.99%. The viscosity of the crude oil decreases, and its flowability is further enhanced.

Keywords: low-permeability; supercritical CO$_2$ huff-n-puff; permeability; porosity; wettability; viscosity

1. Introduction

In the context of carbon neutrality, the technology of using CO$_2$ for oil extraction has garnered significant attention [1–3]. Compared to other swelling agents, such as nitrogen, deoxygenated air, and reactive water, carbon dioxide is more soluble in crude oil under extraction conditions, providing additional reservoir energy [4–6]. Carbon dioxide can reach a supercritical state at temperatures above 31 °C and pressures of 7.50 MPa. In this state, carbon dioxide exhibits excellent dissolving capabilities for both crude oil and water, leading to an increased oil recovery through mechanisms such as expanding the volume of oil, reducing oil viscosity, lowering oil–water interfacial tension, dissolving-gas-drive, and enhancing core permeability [7–11].

Low-permeability reservoirs in Daqing Oilfield are primarily concentrated in the peripheral fields and the exterior reservoirs of Changyuan Oilfield. These reservoirs are characterized by poor physical properties, low permeability, low movable fluid saturation, poor pore connectivity, and high clay content [12]. Studies have shown that injecting supercritical CO$_2$ into low-permeability reservoirs is an effective method for improving oil recovery in these reservoirs. Additionally, it enables the utilization and geological storage of CO$_2$, thereby mitigating the greenhouse effect [13–15]. However, in practical

applications in Daqing Oilfield, the injection of supercritical CO_2 to enhance oil recovery has not yielded the expected results, limiting the widespread application of this technology. After the injection of supercritical CO_2 into low-permeability reservoirs, CO_2 dissolves in the connate water within the reservoir, forming carbonic acid. Under certain conditions, carbonic acid can react with the minerals in the reservoir, thereby altering the reservoir's physical properties and microstructure to some extent. Moreover, supercritical CO_2 in the reservoir state can not only extract light components from the crude oil but can also dissolve in the oil itself, leading to oil volume expansion and viscosity reduction [16–19].

Rathnaweera et al. [20] studied the impact of supercritical CO_2 and saline water on the mechanical properties of sandstone. The results showed significant dissolution of quartz minerals and dissolution of calcite and siderite in both the supercritical CO_2–water and saline–water systems. This indicates that the chemical dissolution of minerals and rock promotes the collapse of rock pores, leading to damage to the mechanical properties of the rock. Isaka et al. [21] investigated the changes in uniaxial and triaxial mechanical properties of granite under long-term exposure to supercritical CO_2 over two months. They found that changes in the mineral structure of granite were caused by the dissolution of silicate minerals and feldspar minerals, resulting in a decrease in rock strength. The dissolution and precipitation of minerals also affected the corrosive action of supercritical CO_2 on granite, exhibiting time-dependent degradation. Wang Shaopeng [22] and others determined the solubility, density, and volume coefficient of CO_2 in Daqing crude oil and reservoir water at different pressures using the PVT method. The study found that the solubility of CO_2 increased linearly with increasing pressure, and the volume coefficient of the saturated CO_2–oil–water mixture depended on the experimental pressure and the amount of dissolved gas, while it was less influenced by the liquid-phase composition. Li Yuxing [23] conducted experiments on viscosity reduction and solubility of super-heavy oil using supercritical CO_2 and simulated the properties using a fluid equilibrium model. They derived the calculation formulas for the solubility and volume coefficient of supercritical CO_2 in super-heavy oil.

Currently, the characterization of rock porosity evolution under the action of supercritical CO_2 primarily relies on porosity, permeability, or adsorption characteristics. There is insufficient understanding of the dissolution behavior of supercritical CO_2 under high-temperature and high-pressure conditions, a lack of research on other physical properties of rock minerals, and insufficient analysis of mineral compositions in core samples. Therefore, this study is based on laboratory experiments simulating the physical simulation of supercritical CO_2 injection. It focuses on the changes in reservoir properties and crude oil properties before and after the experiments using natural low-permeability core samples. The study quantitatively analyzes the changes in permeability and porosity of the core, investigates the variations in mineral composition, and examines the changes in the hydrocarbon composition of crude oil. Unlike conventional viscosity analysis of extracted crude oil, this study uses the falling ball method to simulate and analyze the viscosity changes of the crude oil under the temperature and pressure conditions of the experiments.

2. Experimental Section

2.1. Materials and Instruments

The low-permeability natural rock cores used in the experiment were obtained from the target block of Daqing Oilfield. The dimensions of the cores were φ2.5 cm × 5 cm, and their main characteristic parameters are shown in Table 1. The crude oil used in the experiment was Daqing Oilfield's crude oil, with a surface density of 0.8268 g/cm^3 (20 °C, 0.101 MPa) and a viscosity of 4 mPa·s (71 °C, 0.101 MPa). The water used in the experiment was laboratory-prepared simulated formation water with a salinity of 12,500 mg/L and predominantly contained sodium ions. The water type was $NaHCO_3$. The CO_2 used in the experiment was provided by Qingdao China Gas Co., Ltd., with a purity of 99.99%.

Table 1. Characteristic parameters of natural core.

Core Number	Length (cm)	Diameter (cm)	Raw Permeability (10^{-3} μm^2)	Raw Porosity (%)
Z1	5.01	2.51	1.541	12.32
Z2	5.10	2.51	0.431	14.11
Z3	4.98	2.50	0.982	10.72
Z4	5.11	2.50	0.361	11.24
Z5	5.00	2.49	1.425	15.42
Z6	5.00	2.50	0.742	9.88

The QKY-2 Porosity Determination Instrument is manufactured by Hai'an China Co., Ltd. The GASPERM Gas Permeability Measurement Instrument is produced by Vinci Technologies, a company based in Paris France. The Agilent 5973I Gas Chromatography-Mass Spectrometry System is manufactured by Agilent Technologies in the United States. The CHY-ΓΠ Viscometer is a product of Brookfield, a company based in the United States. The D8 Advance X-ray Diffraction Instrument is manufactured by Bruker, a company from Berlin, Germany. The OCA25 Contact Angle Measurement Instrument is produced by Dataphysics, a company based in Berlin, Germany. The displacement experiment equipment mainly includes an ISCO syringe pump (manufactured by Teledyne ISCO, United States, with a flow accuracy of 0.001 mL/min), a temperature- and pressure-resistant piston container, core holders, a hand pump, a temperature-controlled chamber, a data acquisition device, pressure gauge, etc. For more detailed information, please refer to Figure 1.
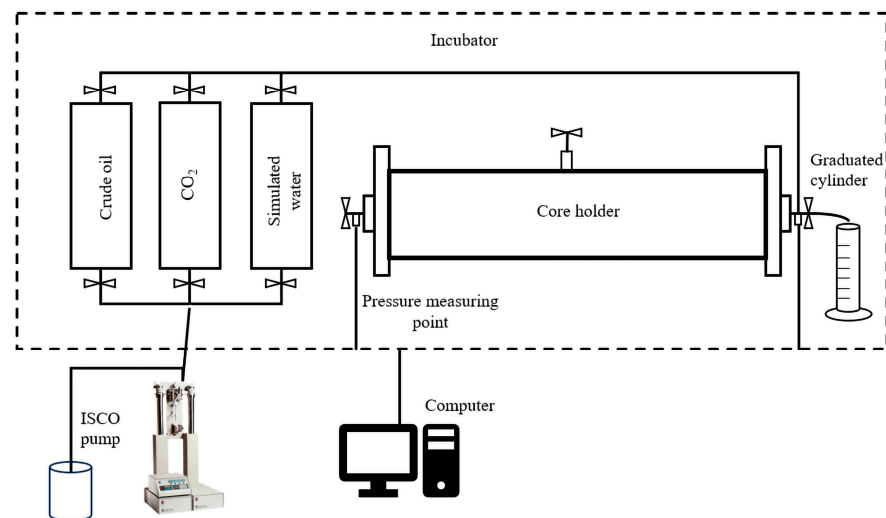
Figure 1. Displacing experimental device.

2.2. Experimental Method

To investigate the changes in the physical properties of the porous media and fluids in low-permeability cores after supercritical CO_2 flooding, the following experimental procedure was designed: (a) The natural rock cores were first washed with xylene and then dried in a temperature-controlled chamber at 71 °C for 24 h. After drying, the cores were weighed and sampled for scanning electron microscope (SEM) observation to obtain the initial microstructure of the cores.

(b) The dried natural rock cores were subjected to a permeability measurement using the gas permeability measurement instrument and porosity determination using the porosity determination instrument. Subsequently, a vacuum was applied for 24 h to achieve a pressure below 1 Pa, followed by saturation with water. (c) The prepared rock cores were placed in core holders, connected with pipelines, and checked for airtightness. The temperature of the temperature-controlled chamber was set to 71 °C. After a thermal stabilization

period of 24 h, the cores were saturated with oil at a rate of 0.01 mL/min. (d) Supercritical CO_2 huff-n-puff experiments were carried out on natural cores. CO_2 was injected into the core gripper at an injection pressure of 16 MPa for 5 min to ensure the internal stability of the core gripper at 16 Mpa, and then the valves at both ends of the core gripper were closed. After 24 h of braising, the liquid was extracted from the same end of the core gripper and huff-n-puff was repeated for 3 rounds.

(1) Determination of permeability and porosity of natural rock cores before and after the experiment.

After drying the natural rock cores before and after the experiment, the permeability and porosity are measured using gas permeability measurement instruments and gas porosity determination instruments. This provides information about the changes in the physical properties of the natural rock cores before and after the supercritical CO_2 flooding experiment. (To reduce experimental errors, ensure that each rock core is measured for the same duration when using the gas permeability measurement instrument and porosity measurement instrument).

(2) Determination of the mineral composition of natural rock cores before and after the experiment.

Before and after the experiment, the natural rock cores are dried, sliced, and ground into powder. X-ray diffraction analysis is conducted to determine the mineral composition of the natural rock cores before and after the supercritical CO_2 flooding.

(3) Determination of wettability of natural rock cores before and after the experiment.

After drying the natural rock cores, prepare 2 mm thick slices and measure the water contact angle to assess the wettability changes before and after the huff-n-puff experiment. Prior to the contact angle measurement, ensure that the rock core slices and water are thermally stabilized at 71 °C for 1 h.

(4) Determination of total hydrocarbon composition in crude oil.

First, the intermediate container is cleaned, and 100 mL of the crude oil sample is poured into it. The temperature of the temperature-controlled chamber is set to 71 °C. After a thermal stabilization period of 24 h, CO_2 is injected into the intermediate container to achieve an internal pressure of 16 MPa. The intermediate container is rotated to ensure sufficient contact between the crude oil and CO_2. After 12 h, the crude oil is extracted, and its structural characterization is performed using a gas chromatography-mass spectrometry (GC-MS) instrument. The temperature program for gas chromatography is as follows: hold at an initial temperature of 50 °C for 10 min, then increase the temperature at a rate of 5 °C/min until reaching 300 °C, and hold for 20 min.

(5) Determination of crude oil viscosity under experimental conditions.

First, the intermediate container is cleaned, and 500 mL of the crude oil sample is poured into it. The viscosity meter temperature is set to 71 °C. After a thermal stabilization period of 1 h, CO_2 is injected into the intermediate container to achieve an internal pressure of 16 MPa. The intermediate container is rotated to ensure sufficient contact between the crude oil and CO_2. After 2 h, the drop time is measured at different drop angles, and the crude oil viscosity is calculated using Equation (1). Five pressure points are simulated, and the viscosity meter is used to measure the changes in the crude oil viscosity under different supercritical CO_2 injection pressure conditions (10 MPa, 12 MPa, 14 MPa, 16 MPa, and 18 MPa). (The ball drop angle and time can be captured by a camera, and the data can be automatically recorded by an information collection system to minimize measurement errors).

$$\mu = kt(\rho_a - \rho_f) \tag{1}$$

t—Ball fall time;
ρ_a—Pellet density;
ρ_f—Crude oil density;
k—Fixed parameter (related to the drop angle of the ball).

3. Results and Discussion

3.1. Changes in Core Permeability before and after Huff-n-Puff

After supercritical CO_2 flooding in low-permeability reservoirs, the physical properties of the natural rock cores can be affected by the presence of supercritical CO_2. The permeability and porosity of the rock cores are essential parameters in this study. The permeability of natural rock cores Z1–Z6 before and after the supercritical CO_2 flooding was determined, and the experimental results are shown in Table 2 and Figure 2.

Table 2. Changes in core permeability.

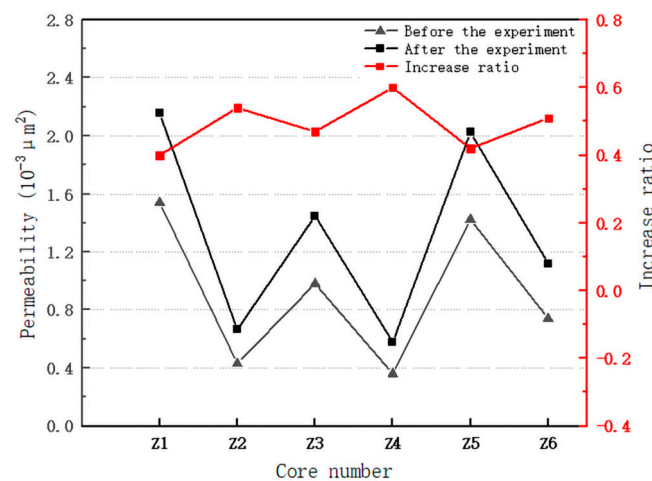| Core Number	Raw Permeability $(10^{-3}\ \mu m^2)$	Post-Experimental Permeability $(10^{-3}\ \mu m^2)$
Z1	1.541	2.157
Z2	0.431	0.664
Z3	0.982	1.449
Z4	0.361	0.578
Z5	1.425	2.025
Z6	0.742	1.122

Figure 2. Permeability change curve.

The injected supercritical CO_2 dissolves in the remaining water within the rock cores, forming carbonic acid. After a prolonged soaking period, the minerals in the rock cores can undergo dissolution. The target zone rock cores contain a significant amount of feldspar and calcite, which readily reacts with carbonic acid, leading to dissolution and the creation of etched pores, thereby increasing the permeability of the rock cores. From Figure 2, it can be observed that the permeability of the natural rock cores undergoes varying degrees of increase after supercritical CO_2 flooding, with an increased ratio ranging from 40% to 60%. Among them, the increase in permeability is relatively small for Z2, Z3, Z4, and Z6 rock cores, with a permeability lower than $1 \times 10^{-3}\ \mu m^2$, while Z1 and Z5 exhibit a greater increase in permeability. This is because compared to rock cores with higher permeability, rock cores with lower permeability have a larger surface area of internal pore solid particles, making the dissolution effect of carbonic acid more pronounced.

3.2. Changes in Core Porosity before and after Huff-n-Puff

After supercritical CO_2 flooding, another property closely related to the permeability of low-permeability natural rock cores, the porosity of the rock cores, exhibits a more pronounced increase. This is mainly due to the injected supercritical CO_2 dissolving in the remaining water within the rock cores, forming carbonic acid, which has a dissolution effect

on the minerals in the rock cores, resulting in etched pores and an increase in the porosity of the rock cores. The specific results can be seen in Table 3. Supercritical CO_2 can not only dissolve the matrix cement and increase the content of small pores but also dissolve medium-sized pores into larger ones. From Table 3 and Figure 3, it can be observed that the porosity of the experimental rock cores increases by 1.06% to 5.68% after supercritical CO_2 flooding. The increase in porosity is not significant for Z1 and Z6, which may be mainly due to the high content of calcite in the rock cores of this area. When calcite is dissolved by acid, the generated Ca^{2+} reacts with the subsequently produced carbonic acid to form secondary precipitation. As a result, the porosity of the natural rock cores initially decreases and then increases during the experimental process, leading to a relatively small overall change in porosity.

Table 3. Changes in core porosity.

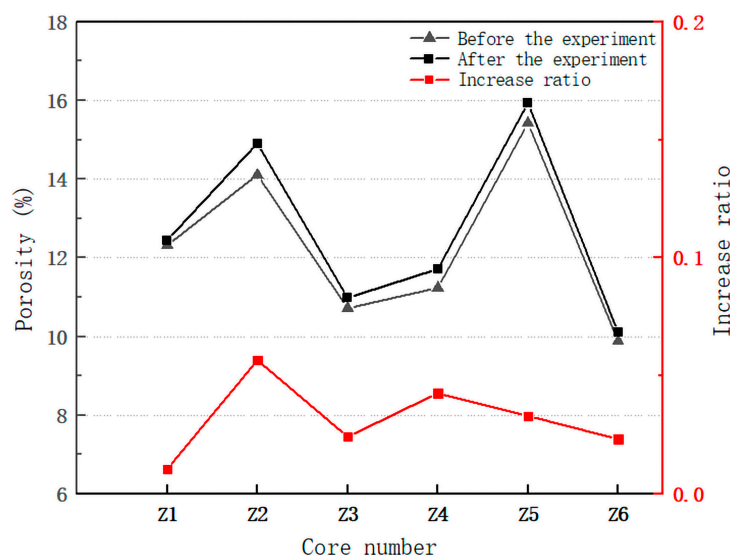| Core Number	Raw Porosity/%	Post-Experimental Porosity/%
Z1	12.32	12.45
Z2	14.11	14.91
Z3	10.72	10.98
Z4	11.24	11.72
Z5	15.42	15.93
Z6	9.88	10.11

Figure 3. Porosity change curve.

As an acidic gas, CO_2 can generate weak acid when in contact with formation water. It can react with certain cementing materials and also inhibit the expansion of some viscosity particles. Additionally, it can react with abundant calcium carbonate present in the formation, forming bicarbonate. This reaction enables the slight dissolution of the rock surface, optimizing the pore structure and enhancing the permeability of the formation. As a result, the rock's fluid flow capacity is improved. This mechanism plays a crucial role in the enhanced oil recovery achieved through supercritical CO_2 injection.

3.3. Changes in Mineral Composition of Natural Core

After prolonged and multiple rounds of supercritical CO_2 flooding, a series of dissolution reactions between carbonic acid and pores, as well as other chemical reactions, result in changes in the mineral composition within the natural rock cores. The changes in the internal mineral composition of the natural rock cores before and after supercritical CO_2 flooding are shown in Table 4.

Table 4. Changes in core mineral composition before and after the experiment.

Core Number	Quartz Content/%		Feldspar Content/%		Calcite Content/%		Other Mineral Content/%	
	Before	After	Before	After	Before	After	Before	After
Z1	43.5	44.7	45.8	44.8	8.5	7.9	2.2	2.6
Z2	42.3	42.7	48.7	47.8	6.2	5.8	2.8	3.6
Z3	46.3	47.2	43.9	42.8	7.3	6.9	2.5	3.1
Z4	45.2	46.3	41.3	39.8	6.4	5.2	7.1	8.7
Z5	41.6	42.5	42.3	41.2	6.9	6.3	9.2	9.9
Z6	42.3	43.5	42.6	41.2	7.9	7.0	7.2	8.3

The natural rock cores in this area are mainly composed of quartz, feldspar (plagioclase + potassium feldspar), and calcite. From Table 4, it can be observed that before the experiment, the dominant component in the rock cores of this area was feldspar (plagioclase + potassium feldspar), accounting for approximately 50% of the total mineral content. Quartz was the second most abundant mineral, accounting for approximately 30–40% of the total mineral content, while calcite had the lowest abundance, accounting for approximately 10% of the total mineral content. The remaining minerals were other minerals (siderite + dolomite + clay). After supercritical CO_2 flooding, the content of quartz in the natural rock cores remained relatively stable or slightly increased. This is because quartz is not significantly involved in the physical and chemical reactions that occur during the experiment. However, the decrease in the content of other reacting components indirectly increases the proportion of quartz. During the experiment, carbonic acid mainly reacts with feldspar (plagioclase + potassium feldspar) and calcite, leading to a varying degree of reduction in the content of feldspar (plagioclase + potassium feldspar) and calcite within the natural rock cores. After supercritical CO_2 flooding, various changes occur within the natural rock cores, resulting in an increase in the proportion of other minerals.

3.4. Change in Oil–Water Wettability of Natural Core

After prolonged and multiple rounds of supercritical CO_2 flooding, the oil–water wettability of the natural rock cores changes due to the dissolution effect of carbonic acid on the porous medium. The variation in wettability of natural rock core Z4 before and after supercritical CO_2 flooding is shown in Figure 4.

(**a**) Before the experiment

(**b**) Post-experiment
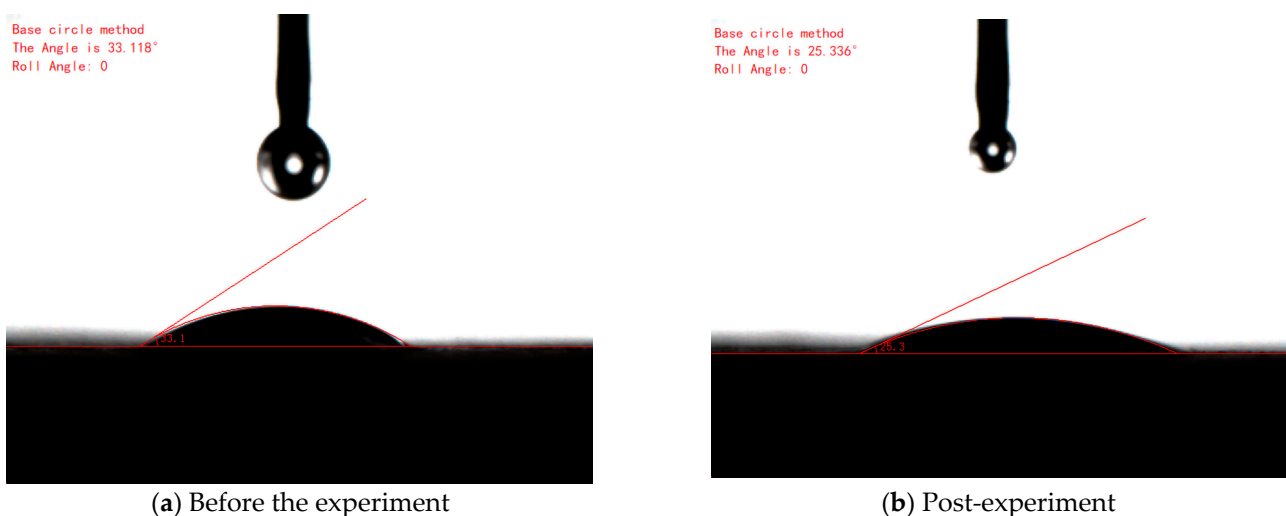
Figure 4. Z4 core water-phase wetting angle.

According to Figure 4, it can be observed that the water-phase contact angle of natural rock core Z4 decreased from 33.118° before the experiment to 25.336° after the experiment, representing a reduction of 23.5%. The strength of hydrophilicity varies among

different minerals. In the studied block, the major minerals in the natural rock cores are quartz, feldspar (plagioclase + potassium feldspar), and calcite, with different degrees of hydrophilicity. The hydrophilicity of feldspar (plagioclase + potassium feldspar) and calcite is similar, while quartz exhibits higher hydrophilicity compared to these two minerals. The influence of the remaining minerals (siderite + dolomite + clay) can be neglected due to their relatively small proportion.

After prolonged and multiple rounds of supercritical CO_2 flooding, carbonic acid reacts with the internal pores of the rock cores, primarily involving feldspar (plagioclase + potassium feldspar) and calcite. As the content of these two minerals decreases, the content of quartz and other minerals (siderite + dolomite + clay), which do not participate in the reaction, increases. Due to the strong hydrophilicity of quartz, the natural rock core exhibits an enhancement in hydrophilicity after undergoing supercritical CO_2 flooding. Furthermore, when CO_2 dissolves in formation water, the resulting carbonic acid reacts with the rock, leading to the removal of the oil film on the rock's surface. As CO_2 continues to dissolve in the formation water, the aqueous CO_2 solution adsorbs on the surface of rock particles, forming a thin film of CO_2 solution, which alters the wettability of the rock.

3.5. Microscopic Changes in Porous Media

Based on the analysis above, it is evident that after the injection of supercritical CO_2 into the rock core pores, the carbonic acid formed by the dissolution of supercritical CO_2 in water reacts with the minerals in the rock core. This reaction leads to an increase in the permeability and porosity of the rock core. To further investigate the changes in the rock core pores after supercritical CO_2 injection, electron microscopy scans were conducted on sliced samples of all the experimental rocks. The results, using rock core Z2 as an example, are shown in Figure 5.
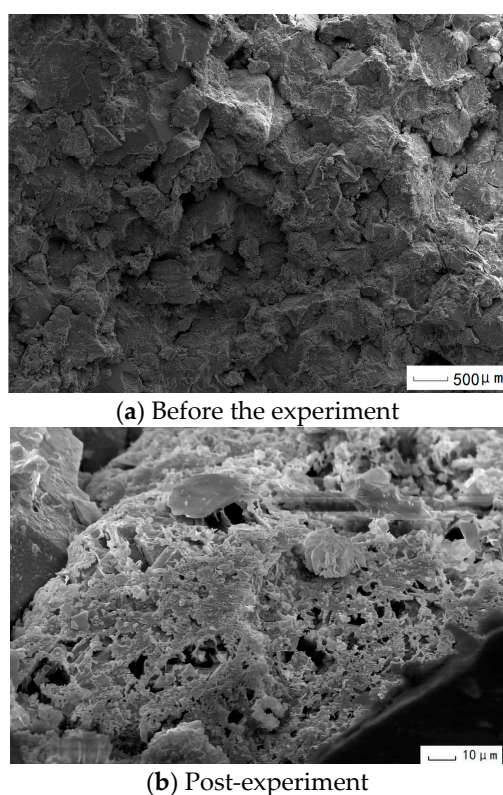

(**a**) Before the experiment

(**b**) Post-experiment

Figure 5. Comparison of micromorphology of natural core Z2 before and after the experiment.
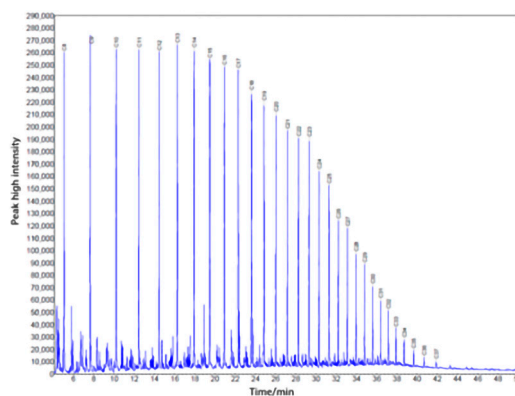
From Figure 5a, it is evident that the internal porous medium of the rock core, without undergoing supercritical CO_2 flooding, is relatively dense, with poor connectivity and limited development of pores between particles. However, upon observing Figure 5b, it

becomes clear that after supercritical CO_2 flooding, numerous small pores have appeared on the surface of the rock core particles. These small pores are formed due to the dissolution of the rock core particles by the carbonic acid generated during the supercritical CO_2 flooding process.

Furthermore, as a result of the reaction between calcite and the formed carbonic acid, the clay minerals that were bound by the cemented calcite undergo detachment. This causes the rock core to become more porous, improves connectivity, and facilitates the development of intergranular pores. Consequently, the permeability and porosity of the rock core increase.

3.6. Changes in the Properties of Crude Oil

To study the extraction characteristics of supercritical CO_2 on crude oil, a simulated contact reaction between crude oil and supercritical CO_2 was conducted under experimental conditions. After sufficient contact between crude oil and supercritical CO_2 under the experimental conditions, a comparison of the crude oil's total hydrocarbon composition before and after the experiment was measured using a gas chromatograph, as shown in Figure 6.

(**a**) Total hydrocarbon distribution of crude oil before experiment.
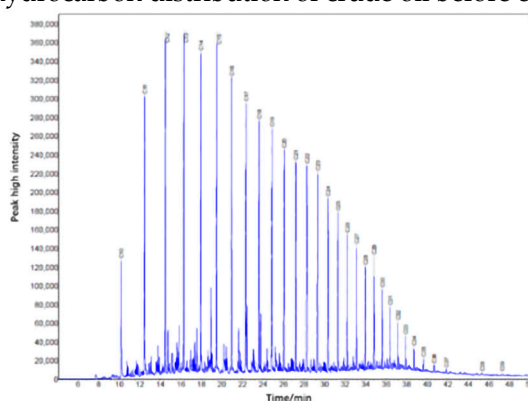
(**b**) Total hydrocarbon distribution of crude oil after experiment.

Figure 6. Change of total hydrocarbon of crude oil.

From Figure 6a, it is evident that the carbon number distribution of the crude oil sample in the experimental block is mainly concentrated in the range of C_8–C_{17}, with approximately 54.33% of the content being C_{17} and below. By comparing the two data graphs, it is clear that the crude oil undergoes significant changes in its total hydrocarbon composition due to the extraction effect of supercritical CO_2. Lighter components such as C_8–C_{10} are extracted by supercritical CO_2, resulting in a decrease of approximately 14.6% in their content. Specifically, C_8 and C_9 show a reduction of nearly 100%. As a result, heavier components such as C_{16}–C_{39} experience an increase in content by 6.99%. Therefore,

supercritical CO_2 can extract light hydrocarbon components from crude oil, which can help improve the oil recovery rate.

The experimental study investigated the variation of crude oil viscosity under different supercritical CO_2 injection pressure conditions (10 MPa, 12 MPa, 14 MPa, 16 MPa, and 18 MPa). The data obtained from the experiment are presented in Table 5 and Figure 7.

Table 5. Crude oil viscosity under different CO_2 injection pressures.

| Injection Pressure (Mpa)	Angle of Drop (°)	Drop Time (s)			Average Time (s)	Viscosity (mPa·s)	Average Viscosity (mPa·s)
		1	2	3			
10	22.5	1.17	1.17	1.17	1.17	3.94	4.64
	45	0.75	0.76	0.76	0.75	4.73	
	67	0.61	0.61	0.61	0.61	5.25	
12	22.5	1.19	1.20	1.19	1.19	4.02	4.49
	45	0.70	0.70	0.70	0.70	4.40	
	67	0.59	0.58	0.59	0.59	5.05	
14	22.5	1.14	1.14	1.14	1.14	3.84	4.34
	45	0.69	0.69	0.69	0.69	4.34	
	67	0.57	0.56	0.56	0.56	4.85	
16	22.5	1.12	1.12	1.13	1.12	3.79	4.26
	45	0.70	0.71	0.71	0.71	4.45	
	67	0.53	0.53	0.53	0.53	4.56	
18	22.5	1.08	1.08	1.08	1.08	3.64	3.96
	45	0.61	0.61	0.62	0.61	3.85	
	67	0.51	0.51	0.51	0.51	4.39	
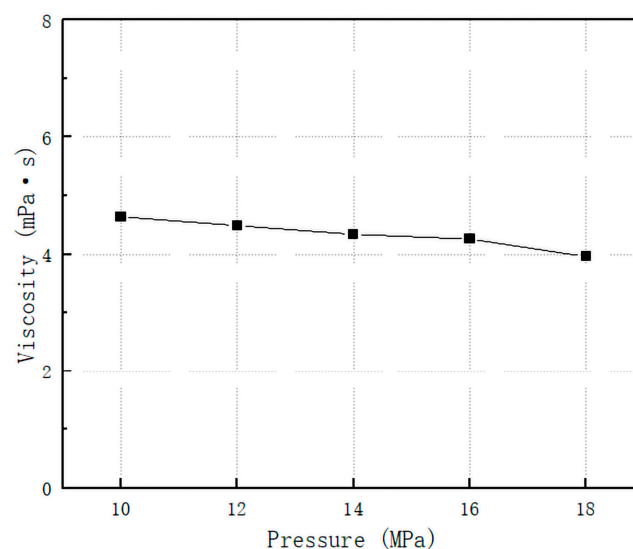
Figure 7. Crude oil viscosity under different CO_2 injection pressures.

From Table 5 and Figure 7, it is evident that supercritical CO_2 has a viscosity-reducing effect on crude oil. Consequently, the oil–water mobility ratio in the reservoir decreases after injecting supercritical CO_2. The reduction in the oil–water mobility ratio can enhance sweep efficiency, thereby increasing the oil recovery rate. Therefore, it can be observed that through supercritical CO_2 flooding, the light hydrocarbon components of the reservoir's crude oil are extracted, leading to a decrease in crude oil viscosity. This improves the fluid

properties of the crude oil and enhances its flowability, which is beneficial for reducing residual oil saturation and, consequently, increasing the oil recovery rate.

Furthermore, the dissolution of CO_2 in crude oil reduces its viscosity. Therefore, the oil–water mobility ratio in the reservoir also decreases after CO_2 injection. The decrease in the oil–water mobility ratio can enhance sweep efficiency and thus increase the oil recovery rate. Additionally, some data indicate that the viscosity of water increases by more than 20% when CO_2 is dissolved in it [24,25]. With the increased viscosity of water and the decreased viscosity of crude oil, the oil–water mobility ratio is further reduced, which can improve sweep efficiency and ultimately enhance the oil recovery rate through the injection of supercritical CO_2.

3.7. Practical Application

The W119 fault block is located in the Ba County sag of the Jizhong Depression, with a structure resembling a castle-shaped nose on the Wen'an slope—the geological reserves in this block amount to 245.39 million metric tons (Mt). The average porosity of the fault block is 21%, with an average permeability of 20.8×10^{-3} μm^2. The viscosity of the reservoir crude oil is 18.8 mPa·s. Currently, the block has a daily oil production of 16.59 metric tons (t) with a high water cut of 95.59% and a recovery factor of 21.14%. The reservoir exhibits strong heterogeneity, and the main layers have long been the primary production zones. Additionally, the intrusion of bottom water has formed dominant water flow channels, leading to a decreasing effectiveness of water flooding over the years and severely constraining the development of the fault block.

In 2021, CO_2-flooding pilot tests were conducted in two well groups, W119-11 and W119-23. The test wells consisted of two injection wells and twelve production wells. By the end of 2022, a total of 1.8 thousand metric tons (kt) of CO_2 had been injected, resulting in an incremental oil production of 1.2 kt. However, after CO_2 flooding, the reservoir oil and its properties have changed, altering the flow characteristics and displacement mechanism. Due to the high gas–oil ratio, 87% of the shut-in wells are currently out of production in the test area, significantly affecting the development effectiveness of the experimental block.

To address this issue, adjustments were made to the injection parameters and methods of the two injection wells based on laboratory experiments and the dynamic production analysis of the oil wells (see Table 6). After adjusting the injection parameters in the pilot test-well group, the gas–oil ratio decreased to below 400 m/m, and the well opening rate increased to 95%. The daily oil production increased from 5.6 t to 15 t, resulting in a cumulative incremental oil of 5760 t. The recovery factor in the swept area improved by 0.23%, and the injection pressure increased by 3.5 MPa. By optimizing the injection method and reducing the amount of CO_2 injected, the cost per ton of oil was reduced by 10.2%.

Table 6. Comparison of injection parameters before and after adjustment in the test area.

Pound Sign	Before the Adjustment		After the Adjustment			
	Injection Volume/(t·d^{-1})	Injection Mode	Injection Volume/(t·d^{-1})		Injection Mode	Water-Air Ratio
			Supercritical CO_2	Water		
W119-11	30	Continuous gas injection	15	10	Alternation of water and air	1.5:1
W119-23	30		20	10		1:1

4. Conclusions and Suggestions

To address the lack of clear understanding regarding the changes in reservoir porous media and the fluid properties induced by supercritical CO_2 flooding, a study was conducted based on physical simulation experiments of supercritical CO_2 flooding on low-permeability natural rock cores. The aim was to investigate the variations in reservoir microstructure, permeability, porosity, mineral composition, and fluid composition before and after the experiments. The study analyzed the interaction patterns between supercriti-

cal CO_2 and the original reservoir, aiming to provide insights for enhancing development efficiency in low-permeability reservoirs in the Daqing Oilfield through the use of supercritical CO_2 flooding. However, this study mainly focuses on the changes in porosity, permeability, and mineral composition, and the experimental scope is relatively narrow. In future research, additional experiments related to capillary pressure and other relevant factors will be included to gain a more comprehensive understanding of reservoir dynamics and provide guidance for field operations.

(1) After prolonged supercritical CO_2 flooding, low-permeability natural rock cores exhibit a significant increase in permeability and porosity. This is primarily due to the reaction between the injected CO_2 and the simulated formation water, resulting in the formation of carbonic acid. Carbonic acid, being a weak acid, slowly acidifies the interior of the natural rock cores through its unique chemical properties. This reaction causes various minerals to react, ultimately leading to changes in the internal structure of the natural rock cores, improving the pore structure and physical properties. Therefore, supercritical CO_2 huff-n-puff can enhance the permeability of the formation and reduce gas injection pressure. However, reducing the injection pressure may result in a smaller affected area. Therefore, in subsequent injection adjustment processes, the addition of blocking agents should be considered for sealing off larger pathways and improving gas sweep efficiency.

(2) Under the erosive action of supercritical CO_2, the wettability of natural rock cores also changes, with increased inherent hydrophilicity. This is because different natural minerals exhibit varying wettability towards oil and water. Under the erosive action of supercritical CO_2, the content of less hydrophilic minerals like feldspar and calcite decreases, while the content of more hydrophilic quartz thus increases. As a result, the overall change in the physical properties of the natural rock cores is an enhancement in water-phase wettability. It is worth considering a transition from injecting pure supercritical CO_2 to alternating huff-n-puff with supercritical CO_2 and water injection, which can help achieve cost reduction objectives.

(3) Due to the decrease in the content of feldspar (plagioclase + potassium feldspar) and calcite, which participate in the erosive reaction, the proportion of quartz and other minerals not involved in the reaction significantly increases.

(4) By observing the microscopic morphology of the internal porous media of the rock cores before and after supercritical CO_2 flooding, we can observe that the pre-experiment porous media exhibits characteristics such as density, poor connectivity, and underdeveloped intergranular porosity. However, after the experiment, the porous media showed evident erosive phenomena, displaying loose, improved connectivity, and well-developed intergranular porosity, indicating favorable physical properties.

(5) Supercritical CO_2 exhibits a significant extraction effect on the experimental oil sample. After the flooding experiment, there are noticeable changes in the total light hydrocarbon components of the oil, with a decrease of approximately 14.6% in components such as C_8–C_{10} and an increase of 6.99% in heavier components such as C_{16}–C_{39}. Under the experimental conditions, the viscosity of the oil also decreases to a certain extent, indicating that supercritical CO_2 has a viscosity-reducing effect on the oil.

Therefore, in the field application of injecting supercritical CO_2 to enhance oil recovery, it is necessary to analyze the relationship between dissolution and extraction based on the interaction mechanism between supercritical CO_2 and crude oil (C) in conjunction with the reservoir pressure and temperature conditions. Optimal parameters for supercritical CO_2 huff-n-puff should be selected to improve the effectiveness of the technical application.

Using laboratory high-pressure experimental methods, the study investigated the changes in crude oil properties after supercritical CO_2 dissolution and quantitatively evaluated the variations in formation water and rock properties following CO_2 dissolution. It was found that after CO_2 dissolved in formation water, the pH of the water became acidic, leading to the rapid dissolution of reservoir minerals. As a result, the formation permeability increased by 40–60%, porosity increased by 1.06–5.68%, and the water contact angle decreased by 23.5%. The dual improvement of CO_2 on both crude oil and reservoir

properties enhanced the oil's ability to flow within the formation, providing a theoretical basis for the development of heavy oil and low-permeability reservoirs.

In the CO_2 huff-n-puff pilot test wells of the W119 block, the development performance deteriorated after injecting 1.8×10^3 metric tons of carbon dioxide. Through laboratory experiments and dynamic analysis, adjustments were made to the injection parameters and methods, resulting in a daily oil production increase of 9.4 metric tons and effectively improving the development performance. This provides technical reserves for the design and dynamic adjustment of the injection and production parameters for the subsequent industrial-scale promotion of CO_2 flooding, with significant lessons and reference value.

Author Contributions: Methodology, G.Q.; Formal analysis, X.L.; Data curation, B.L.; Writing—original draft, X.T.; Funding acquisition, Y.L. All authors have read and agreed to the published version of the manuscript.

Data Availability Statement: Data sharing not applicable.

References

1. Meng, C.; Zhigang, Y.; Ming, Z. Progress and Prospect of CCUS-EOR Engineering Technology. *Pet. Sci. Technol. Forum* **2023**, *42*, 49–56.
2. Song, X.; Wang, F.; Ma, D.; Gao, M.; Zhang, Y. Progress and prospect of carbon dioxide capture, utilization, and storage in CNPC oilfields. *Pet. Explor. Dev.* **2023**, *50*, 206–218. [CrossRef]
3. Hill, L.B.; Li, X.C.; Wei, N. CO_2-EOR in China: A comparative review. *Int. J. Greenh. Gas Control.* **2020**, *103*, 103173. [CrossRef]
4. Li, B.; Bai, H.; Li, A.; Zhang, L.; Zhang, Q. Experimental investigation on influencing factors of CO_2 huff and puff under fractured low-permeability conditions. *Energy Sci. Eng.* **2019**, *7*, 1621–1631. [CrossRef]
5. Min, R. The indissoluble bond between carbon dioxide and oil. *Pet. Knowl.* **2016**, *05*, 8–9.
6. Qin, J.; Han, H.; Liu, X. Application and enlightenment of carbon dioxide flooding in the United States of America. *Pet. Explor. Dev.* **2015**, *42*, 209–216. [CrossRef]
7. Abedini, A.; Torabi, F. On the CO_2, storage potential of cyclic CO_2, injection process for enhanced oil recovery. *Fuel* **2014**, *124*, 14–27. [CrossRef]
8. Jiang, H.; Shen, P.; Lu, Y.; Jiang, L.; Luo, J. Research on the current situation of CO_2 enhancing oil and gas recovery in the world. *Spec. Oil Gas Reserv.* **2010**, *17*, 5–10+120.
9. Zhao, L.; Jiang, E.; Wang, S.; Luo, Q.; Li, B.; Zhu, D.; Bai, H. Effect of carbon dioxide injection on mineral and pore structure in low permeability reservoir. *Oilfield Chem.* **2021**, *38*, 659–664+670.
10. Wang, X.; Zhang, Y.; Yan, X.; Wang, H.; Zhao, Y.; Tian, M.; Wang, W.; Wang, L.; Guo, Y. Analysis of supercritical carbon dioxide extraction on crude oil. *Oilfield Chem.* **2023**, *40*, 317–321.
11. Zhang, M.; Wang, L.; Cui, Q.; Hu, Y.; He, S. Experimental study on reservoir physical property change of carbon dioxide flooding. *World Pet. Ind.* **2023**, *30*, 90–96.
12. Liu, J.; Li, L.; Gao, M. Interaction of CO_2 and crude oil in low permeability reservoir. *Oilfield Chem.* **2021**, *38*, 464–469.
13. Chen, X.; Fan, Y. Study on CO_2 huff and puff technology in tight reservoir. *Petrochem. Ind. Appl.* **2021**, *40*, 8–12.
14. Shi, L. Damage characteristics of CO_2 huff and huff asphaltene deposits to reservoirs in tight sandstone reservoirs. *Oilfield Chem.* **2022**, *39*, 343–348.
15. Li, M.; Shan, W.; Liu, X.; Shang, G. Laboratory study on miscible oil displacement mechanism of supercritical carbon dioxide. *Acta Petrolei Sinica* **2006**, *27*, 80–83.
16. Wang, Q.; Yang, S.; Han, H.; Kun, Q.; Wang, L. Impact of CO_2 displacement methods on changes in physical properties of ultra-low permeability sandstone reservoirs. *J. China Univ. Pet. Ed. Nat. Sci.* **2020**, *44*, 124–133.
17. Zhou, T.; Liu, X.; Yang, Z.; Li, X.; Wang, S. Experimental analysis on reservoir blockage mechanism for CO_2 flooding. *Pet. Explor. Dev.* **2015**, *42*, 502–506. [CrossRef]
18. Sun, H.; Zhu, Y.; Wei, Y.; Gao, Y. Influence mechanism of acidification on oil recovery during CO_2 flooding. *Lithol. Reserv.* **2020**, *32*, 136–142.
19. Xia, H.; Xu, Y. Study on the Mechanism and Application of CO_2 Flooding in Low Permeability Reservoirs. *Contemp. Chem. Ind.* **2017**, *46*, 471–474.
20. Rathnaweera, T.D.; Ranjith, P.G.; Perera, M.S.A.; Haque, A.; Lashin, A.; Al Arifi, N.; Chandrasekharam, D.; Yang, S.Q.; Xu, T.; Wang, S.H.; et al. CO_2-induced mechanical behaviour of Hawkesbury sandstone in the Gosford basin: An experimental study. *Mater. Sci. Eng. A* **2015**, *641*, 123–137. [CrossRef]

21. Isaka, B.L.A.; Gamage, R.P.; Rathnaweera, T.D.; Perera, M.S.A.; Chandrasekharam, D.; Kumari, W.G.P. An influence of thermally-induced micro-cracking under cooling treatments: Mechanical characteristics of Australian granite. *Energies* **2018**, *11*, 1338. [CrossRef]

22. Wang, S.; Hou, J.; Zhao, F. Solubility of CO_2 in oil-water mixture and density of saturated CO_2 oil-water. *J. Xi'an Shiyou Univ. Nat. Sci. Ed.* **2012**, *27*, 39–42+57+8.

23. Li, Y.; Zhang, J.; Li, M. Study on Supercritical CO_2 Solubility in Heavy Oil and Heavy Oil Formation Volume Factor. *Sci. Technol. Eng.* **2013**, *13*, 53–57.

24. Lu, J. Numerical Simulation Study of CO_2 Huff and Puff about the Laws on the Control of Water in the Horizontal Wells of Heavy Oil. Ph.D. Thesis, China Petroleum of University, Beijing, China, 2016.

25. Lu, X.; Lu, P. Mechanism and application status of enhancing oil recovery by CO_2 immiscible flooding. *Pet. Geol. Eng.* **2007**, *02*, 58–61.